Supplementary Material

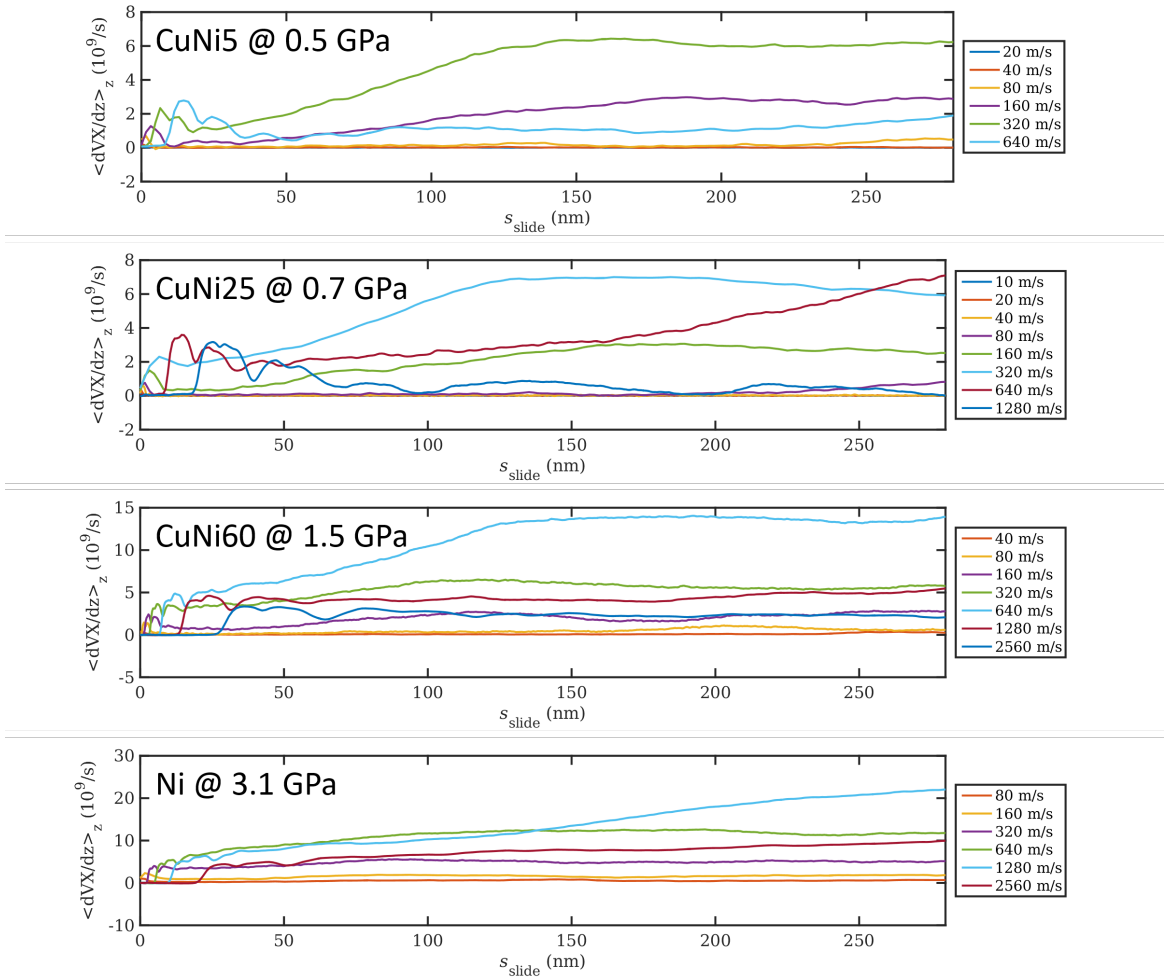

Figure S1: The shear strain rate, averaged over the depth of the sample excluding the near-surface 2 nm and the lower region containing the fine-grained layer, as a function of sliding distance for all simulated systems.

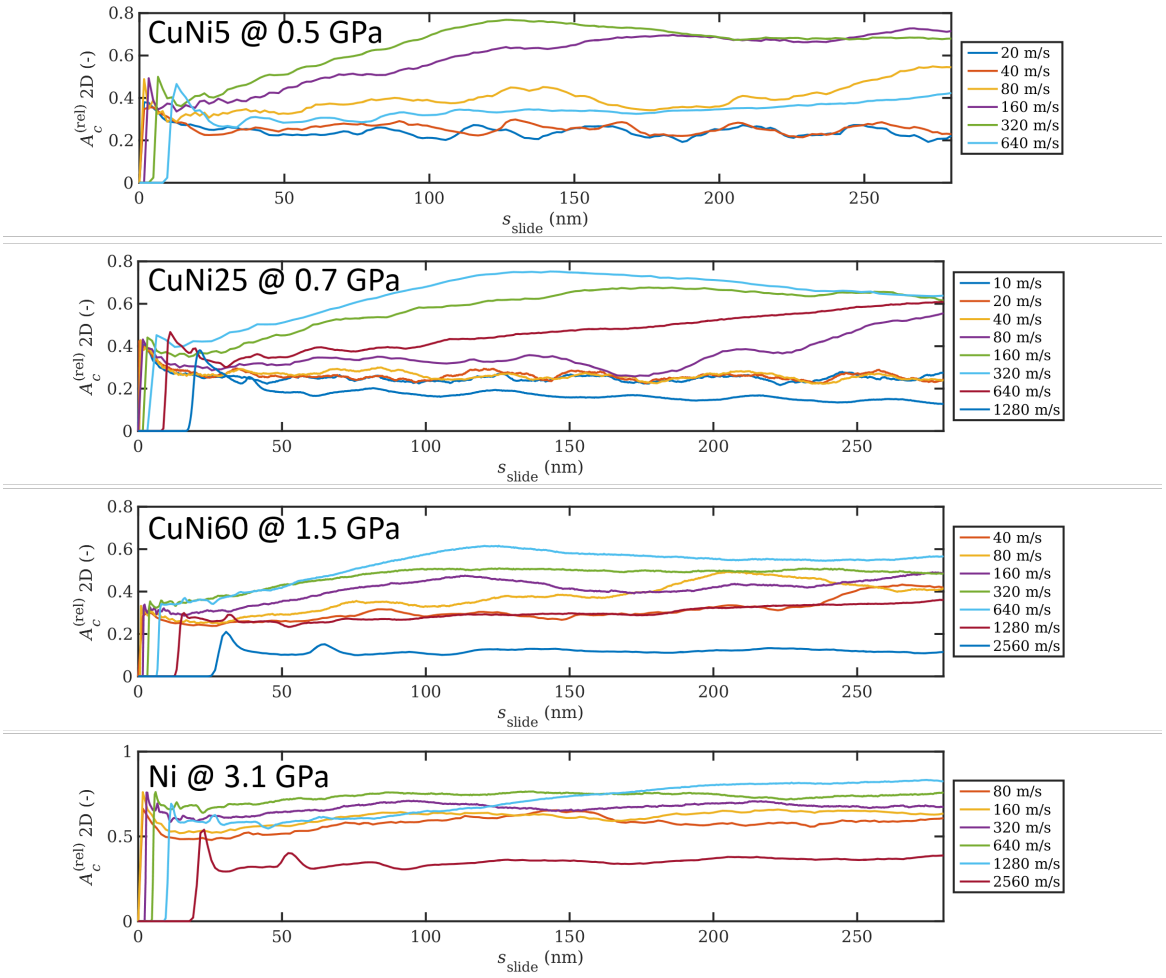

Figure S2: The relative projected real contact area as a function of sliding distance for all simulated systems.

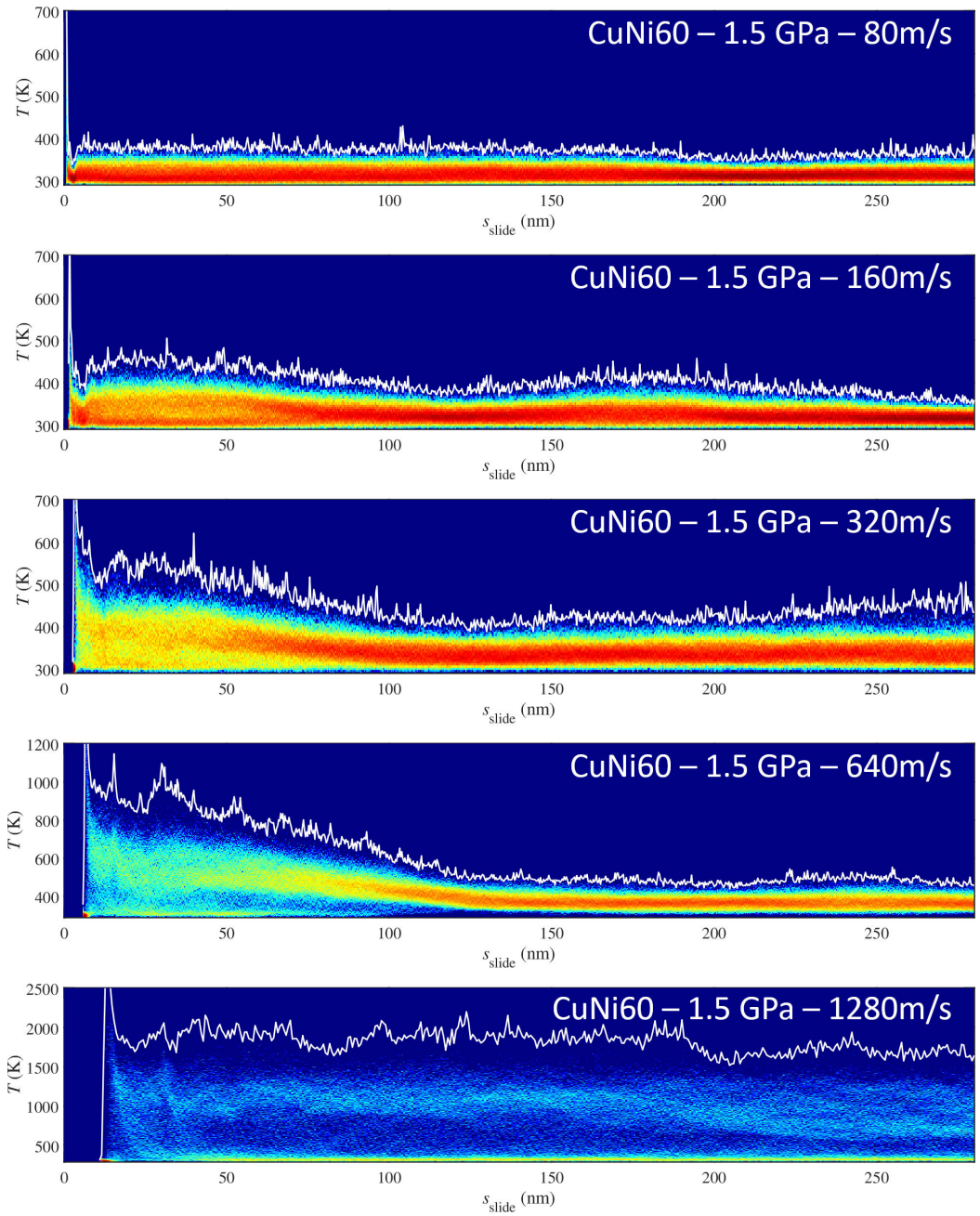

Figure S3: The surface temperature distributions for CuNi60 as a function of sliding distance. Every column of pixels corresponds to the logarithm of the normalized histogram of the surface temperature distribution. The solid white curves denote the maximum recorded temperature values. Note that the lowest two panels have different ordinate axis scaling than the others.

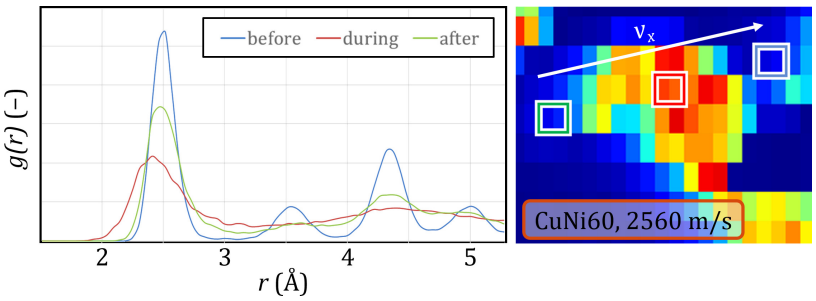

Figure S4: Three radial distribution functions $g(r)$ of near-surface regions of $4\times4\times2$ nm^3 ($\sim$ 3000 atoms) in CuNi60@2560 m/s before (blue), during (red), and after (green) asperity contact. The regions are marked in the zoomed-in surface temperature plot on the right. The respective curves correspond to a crystalline fcc structure, a liquid, and a structure in the process of recrystallization.

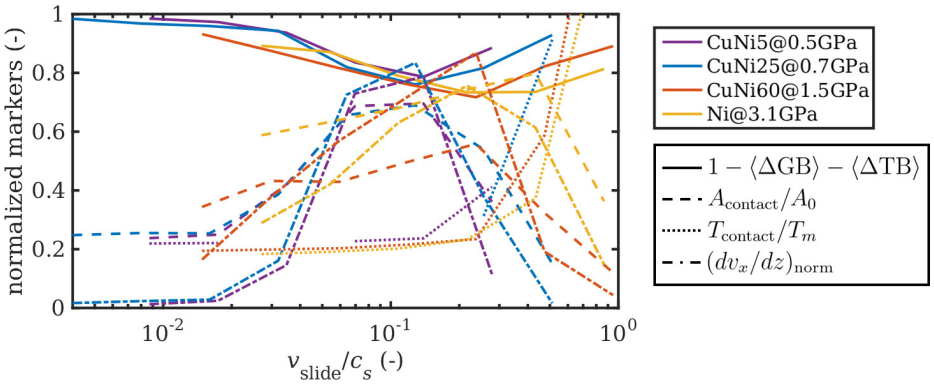

Figure S5: "Precursor" of the master plot in Fig. 6. Microstructural integrity $1-\langle\Delta\mathrm{GB}\rangle-\langle\Delta\mathrm{TB}\rangle$, the normalized real contact area A_c/A_0, the homologous contact temperature T/T_m, and the bulk shear strain rate normalized by ideal Couette flow, $(dv_x/dz)_{\mathrm{norm}}$, as a function of the sliding speed normalized by the speed of sound, v_{slide}/c_s. Here with alloy-resolved curves extracted from the data in Fig. 5, which were then aggregated and simplified to yield Fig. 6.

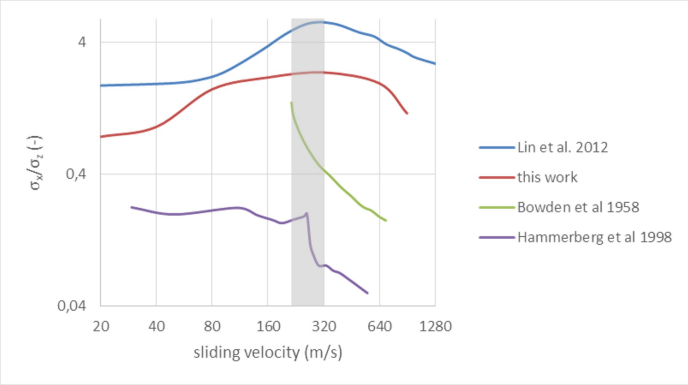

Figure S6: Comparison of the friction stress divided by the normal pressure of CuNi5 at 0.5 GPa (our data) with results from Refs.[28] (Cu vs steel), [44] (Cu vs Cu), and [45] (Cu vs Fe). Although the studies are quite different in nature and conditions, there exists a striking agreement on the narrow velocity range (gray band) above which the friction decreases with sliding speed. In the experimental study by Bowden *et al.* from the late 1950s, a steel ball was suspended in a magnetic field and rotated quickly. It was then brought into contact with three copper plates (one of which is spring-loaded), and the friction decelerates it to the point of seizure at the top left end of the green curve. It must therefore be kept in mind that these data come from one experiment rather than from a series of equilibrated and averaged test results. The study of Hammerberg *et al.* [44] is an early 2D MD-simulation conducted at a very high pressure of 30 GPa, which explains the very low ratio below 0.25. However, it shows the most dramatic decrease in friction just below 300 m/s. The blue curve from Lin *et al.* [45] is a 3D MD study with a small (60k atoms) system thermostatted to 0 K and the Cu–Fe interaction taken directly from the same potential by Bonny that we use in this work [49], which implies a sliding process under UHV and leads to very high lateral forces.